Chapter 12
Vortex Generation by Phase-Controlled Structure-Borne Traveling Waves in a Submerged Beam: A PIV/PTV Fluid–Structure Interaction Study

Rachel Cole, Samikhshak Gupta, Rohit S. Pandhare, and Vijaya V. N. Sriram Malladi

Abstract This work investigates the transfer of mechanical energy from structure-borne traveling waves (TWs) in a slender beam to the surrounding fluid, with a focus on the resulting vortex dynamics. An Aluminum 6061 beam was immersed in water and excited using dual electrodynamic shakers with a controlled phase offset to generate steady traveling waves. Modal testing was employed to identify natural frequencies and establish traveling-wave conditions, while particle tracking velocimetry (PTV) captured near-body flow fields. The PTV measurements resolved coherent vortex formation and fluid motion around the beam, revealing alternating vortices that propagated along its length and induced linear flow within adjacent channels. Analysis showed a consistent relationship between wave kinematics and fluid response, with approximately four vortices forming per excitation wavelength. These results establish an experimental framework linking traveling-wave parameters to circulation and fluid transport. The findings highlight the potential of programmable structural waves as a low-maintenance mechanism for fluid mixing, cooling, and propulsion, offering an alternative to mechanically complex pumps, fans, or rotors.

Keywords traveling wave · PTV · SLDV · vortex formation · modal analysis

Introduction

The transportation sector is undergoing a major transition as governments enforce stricter emission standards and consumers demand cleaner alternatives to fossil-fuel vehicles. Electric vehicles (EVs), including hybrid (HEVs) and battery electric vehicles (BEVs), are central to this shift. Since batteries account for nearly one-third of EV costs, ongoing reductions in price are a key enabler of adoption. Forecasts predict EVs will comprise up to 32% of global vehicle sales by 2030, with BEVs dominating the share. This growth intensifies demand for advanced batteries that offer high energy density, fast charging, low weight, and long cycle life. Lithium-ion batteries (LIBs), the prevailing technology, satisfy many of these requirements but remain highly vulnerable to temperature variations [1–4]. Heat generation during charge–discharge cycles [5–7] and exposure to extreme climates accelerate degradation and raise safety risks, most notably thermal runaway [8–10]. Consequently, robust battery thermal management systems (BTMS) are essential to ensure the safety, durability, and efficiency of EVs. Current BTMS strategies are typically classified as air cooling [11–14], single-phase liquid cooling [15–20], or two-phase cooling [21–23]. Early EVs such as the Toyota Prius and Honda Insight employed air cooling, while later designs such as the Chevrolet Volt and Tesla Model S adopted liquid cooling to improve heat dissipation [20–28]. More recently, immersion cooling with dielectric fluids (e.g., mineral oils) has demonstrated superior thermal performance [29–31], lowering peak cell temperatures and stabilizing fluctuations [32]. However, liquid-based systems require auxiliary power to drive pumps, blowers, and fans. These parasitic loads reduce both vehicle range and efficiency. The challenge is therefore not only to regulate temperature effectively but also to do so with minimal additional energy demand.

Rachel Cole · Samikhshak Gupta · Vijaya V. N. Sriram Malladi
Vibrations, Intelligent Testing, & Active Learning of Structures (ViTALS) Group, Department of Mechanical and Aerospace Engineering, e-mail: recole@mtu.edu; sgupta14@mtu.edu; smalladi@mtu.edu

Rohit S. Pandhare
Complex Fluids and Active Matter (CFAM) Group, Department of Mechanical and Aerospace Engineering, Michigan Technological University, Houghton, MI 49931

© The Author(s), under exclusive license to River Publishers 2026

Kristin B. Zimmerman, PhD (eds.), *Computer Vision and SLDV for Structural Dynamics, 2026, Vol. 6*, Conference Proceedings of the Society for Experimental Mechanics Series, https://doi.org/10.13052/rp-9788743814177

To overcome this limitation, researchers have explored energy recovery strategies that repurpose wasted vibrational and thermal energy within vehicles. Energy harvesting approaches—including piezoelectric absorbers [33–40], thermoelectric generators [41–45], and shape memory alloy engines [46–48]–seek to convert otherwise wasted energy into usable power. While current systems face limitations in efficiency and scalability, they suggest a promising direction: integrating harvested energy with fluid circulation to reduce dependence on electrically powered pumps. Such strategies could enhance BTMS efficiency, extend LIB service life, and improve overall EV performance. Building on this concept, the present work introduces a mechanism that harnesses vibrational noise for fluid circulation, thereby reducing parasitic energy losses and advancing sustainable electric mobility [49–54].

Conventional marine propulsors face similar efficiency and maintenance challenges, as they depend on rotating components. A bio-inspired alternative is thrust generation via undulatory motion of finite structures, in which structure-borne traveling waves (TWs) shed momentum into the fluid to produce net propulsion [55–57]. In elastic media, wave behavior depends strongly on boundary conditions: traveling waves transport energy, whereas standing waves localize it spatially. Single-point excitation in finite structures typically excites reflections and standing modes [58, 59]. By contrast, multiple inputs with controlled phase offsets can suppress reflections and bias energy transport, producing hybrid or near-pure TW fields. Although fully reflection-free TWs remain challenging in bounded domains [60], recent advances have demonstrated controlled TW synthesis across various geometries, including strings [58, 61], beams [62–65], cylinders [59], and plates [66–69]. For example, Malladi et al. developed and experimentally validated a model for TW synthesis in one-dimensional beams under varied boundary conditions using piezoelectric actuation [65], while more recent work has demonstrated distributed actuation in slender plates [70]. The ability to tailor TW kinematics in solids has clear implications for underwater propulsion [71, 68, 55] and for emerging applications such as thermal management, offering a pathway to controllable thrust and circulation without reliance on moving parts.

The central gap lies in establishing a measurement-based understanding of how imposed TW motion couples with the surrounding fluid to generate and organize vortices that mediate momentum exchange. In this study, steady, structure-borne TWs are excited in a one-dimensional beam, and the resulting fluid–structure interactions are characterized using particle tracking velocimetry (PTV). These measurements resolve near-body velocity fields and vortex dynamics, enabling direct correlations between TW parameters (frequency, amplitude, wavenumber, and phase speed) and vortex formation at the beam surface. The objective is to quantify circulation, vortex motion, and flow speeds to determine how TW motion governs fluid velocity and propulsive performance. Ultimately, these insights support the development of low-maintenance cooling and propulsion systems that harness programmable structural waves in place of mechanically complex pumps, fans, or rotors.

Underwater Modal Analysis

The experimental setup for modal analysis of a one-dimensional aluminum beam is shown in Figure 1. The test specimen was an Aluminum 6061 beam with dimensions of $381\text{mm} \times 25.4\text{mm} \times 0.794\text{mm}$. The beam was suspended at both ends using 3D-printed clips bonded with epoxy. Each clip featured a narrow attachment section to minimize fluid disturbance and widened at the top to allow bolting to metal support bars. The support bars were connected to horizontally mounted Modal Shop Smart Shakers to provide excitation. The experiments were conducted in a water tank with internal dimensions of $444.5\text{mm} \times 444.5\text{mm} \times 76.2\text{mm}$, filled to a depth of 114.3mm. The beam was positioned laterally at the tank center, with its lower edge 3mm above the tank floor. Proper alignment between the shakers and the beam was maintained to avoid introducing residual stresses during testing [72].

The supporting frame was constructed from 80:20 aluminum extrusions to ensure rigidity and stability of the test apparatus. Response measurements were obtained using a Polytec OFV-353 laser vibrometer sensor head coupled with an OFV-040 scan unit. The scan unit deflected the laser beam within an angular range of $\pm 15^\circ$ in both x and y axes, controlled through analog voltages (0 to $\pm 5\text{V}$) supplied by an OFV-042 scan controller. Data acquisition was managed by an OFV-3001 vibrometer controller, with velocity measurements taken at 75 uniformly distributed points along the beam. To enhance signal quality, reflective tape was applied along the beam surface. Excitation was provided by the suspended shakers using a chirp signal ranging from 0.1–300Hz with an amplitude of 0.0375V Figure 1. The vibrometer acquired data with 10 averages at each measurement location. Sampling was performed at 17067Hz over a duration of 5s, with a Hanning window applied for spectral analysis. A two-force input strategy was implemented, followed by a multi-input multi-output (MIMO) force-feedback test using the same chirp excitation. Data acquisition employed an NI cDAQ-9174 chassis with NI 9263 and NI 9234 I/O modules. The frequency response functions (FRFs) were computed between the shaker input voltages and the corresponding vibrometer velocity outputs and are shown in Figure 2.

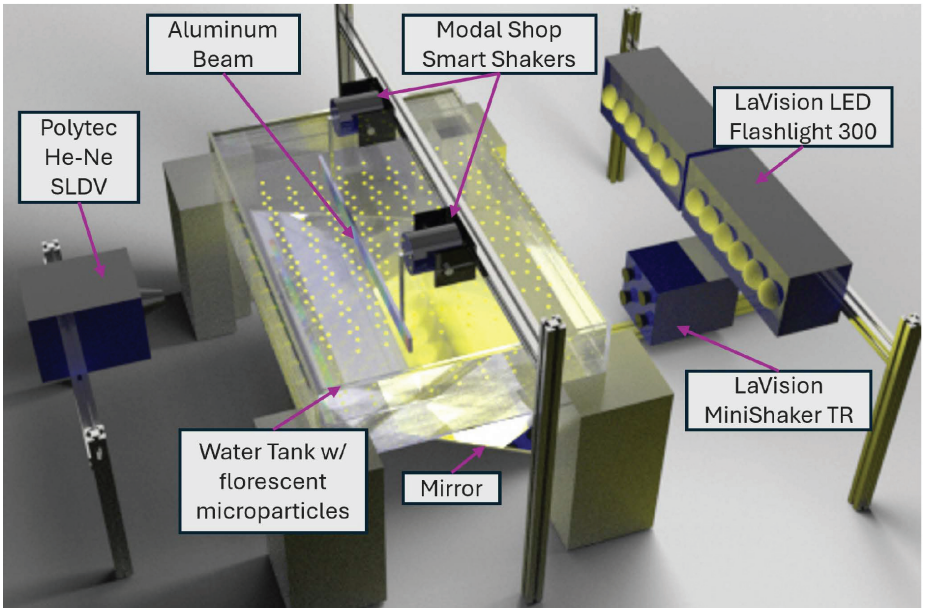

Fig. 1 Schematic Diagram for experimental setup for modal analysis and particle tracking velocimetry of the submerged Al-Beam

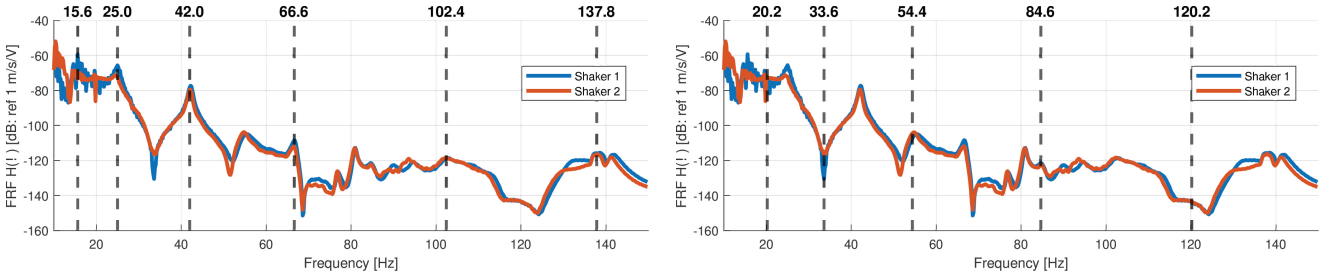

(a) Measured Frequency Response Functions (FRFs) of the aluminum beam with natural frequencies highlighted

(b) Measured Frequency Response Functions (FRFs) of the aluminum beam with traveling wave frequencies highlighted

Fig. 2 Measured Frequency Response Function (FRF) of the submerged aluminum beam

Traveling Wave Generation

Previous studies have shown that elastic structures can support traveling waves when excited by two actuators operated out of phase [73, 65, 74, 75]. The key requirement is to drive the actuators at a mean frequency between adjacent resonances while maintaining a 90° phase shift. This concept was experimentally demonstrated on an aluminum beam using two modal shakers driven at equal amplitudes and a controlled phase offset of 90°. The superposition of their responses produced a structure-borne traveling wave (SBTW). The excitation applied to the two shakers can be expressed as $V_1 = A\sin(2\pi ft)$ and $V_2 = A\sin(2\pi ft \pm \phi)$, leading to a combined input of

$$\textbf{SBTW} = A\sin(2\pi ft) \;\pm\; A\sin(2\pi ft \pm \phi), \tag{1}$$

where A is the excitation amplitude, f is frequency, t is time, and ϕ is the phase difference, ideally 90° for a pure traveling wave. The quality of the generated wave depends primarily on the imposed phase relationship between actuators. In practice, an SBTW often consists of both traveling and standing wave components; reducing the standing contribution enhances wave purity. Malladi et al. [55] proposed a cost function approach to quantify this effect by systematically assessing the strength of the traveling component. The natural frequencies are presented in Figure 2a, while the traveling wave frequencies are shown in Figure 2b and summarized in Table 1.

Table 1 Identified frequencies and corresponding modal or traveling-wave responses.

Frequency	Response Type
15.6 Hz	1st mode shape
20.3 Hz	Traveling wave
25.0 Hz	2nd mode shape
33.55 Hz	Traveling wave
42.0 Hz	3rd mode shape
54.35 Hz	Traveling wave
66.6 Hz	4th mode shape
84.55 Hz	Traveling wave
102.4 Hz	5th mode shape
120.15 Hz	Traveling wave
137.8 Hz	6th mode shape

Particle Tracking Velocimetry

To characterize the flow field generated by the vibrating beam, particle tracking velocimetry (PTV) experiments were conducted. The measurement system consisted of a LaVision MiniShaker TR/2M equipped with four stereo cameras operating at 170 Hz, synchronized with a pulsed LaVision LED-Flashlight 300 for illumination. A 45° mirror was mounted beneath

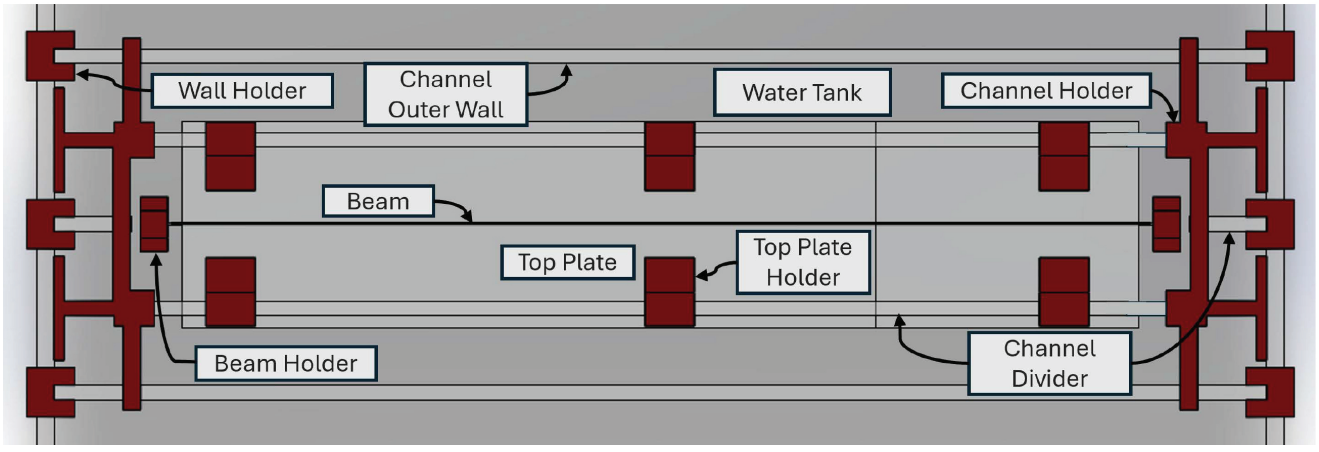

Fig. 3 Top view of underwater beam 19.05 mm channel setup.

the water tank to provide a view normal to the beam's plane of motion. Fluorescent polyethylene microspheres (90–106 μm) were introduced into the water as tracer particles Figure 1. The imaging system was calibrated using a LaVision 309-15 3-D calibration plate illuminated by seven LED light bars, while the water tank was calibrated with the LaVision DaVis volume calibration system, focusing on the water in the space 8 mm below and 9 mm above the center of the beam. To minimize background interference, all overhead lighting was turned off during image acquisition.

Experiments were performed in a double 19.05 mm water channel, with a total width of 117.6 mm from outer wall to outer wall, designed to confine the flow field generated by the vibrating beam Figure 3. The water depth was set to 45 mm, and a top plate was positioned 3 mm above the beam. Before each run, the water was stirred to evenly distribute tracer particles and then allowed to settle to eliminate external disturbances.

During testing, the beam was excited with a 0.4 V sine wave applied to both shakers, with one shaker driven 90° out of phase relative to the other. The system was allowed to stabilize for 10 s before data acquisition began. A total of 600 images were recorded over 3.52 s. Post-processing of the image sets included time-filter subtraction, image pre-processing with masking to isolate the water channel, Shake-the-Box particle tracking, and fine-scale reconstruction.

Results

The focus of this analysis was on excitation frequencies up to 150 Hz. Within this range, the modal analysis identified six natural frequencies for the beam, as shown in the FRF plot in Figure 2. Using the methodology described previously, five traveling waves were also determined, each with the potential to drive fluid motion through the channel setup (Table 1). For the present study, attention was directed to a single traveling wave at 20.3 Hz, where the flow fields around the beam were mapped using the PTV system. Upon visual inspection of both the physical system and the raw PTV images, distinct vortex motion was observed in the inner channel, while linear particle movement was primarily noted in the outer channel. These qualitative observations were later confirmed through processing with the Shake-the-Box algorithm, which detects and tracks the particles over time, as shown in Figure 4. To convert the particle tracks into vector field data, a fine-scale reconstruction was performed on the four regions of the double channel, designated as the inner and outer portions of the upper and lower channels Figure 5. Each of these regions was processed separately to avoid interpolation artifacts across the channel dividers or at the beam location.

In the fine-scale reconstruction, vortices in the Z-direction are clearly visible within the inner channels. These vortices are represented by alternating red and blue regions forming along the beam length, corresponding to positive and negative vorticity, respectively. In contrast, the outer channels display a nearly uniform green field, indicating an absence of strong vortical activity. This observation is consistent with the Shake-the-Box velocity vectors, which show primarily linear particle motion in the outer channels compared to the well-defined rotational motion in the inner channels.

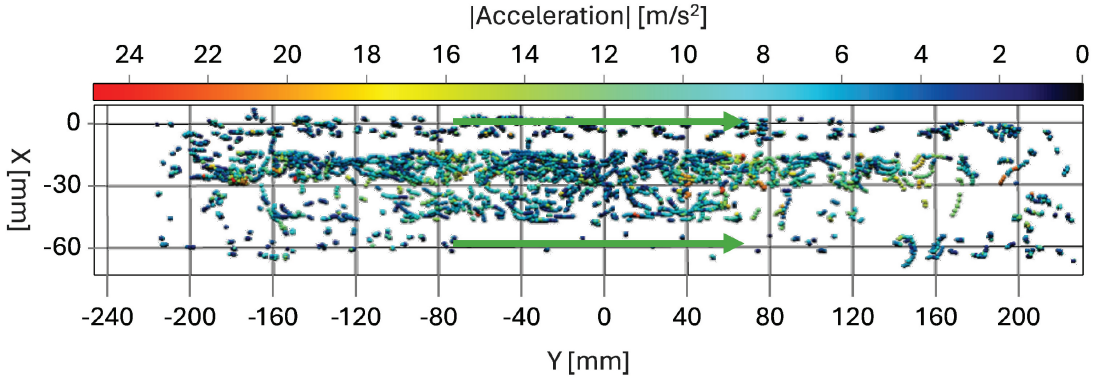

Fig. 4 Shake-the-Box reconstruction of particle motion at 20.3 Hz traveling wave in a 19.05 mm channel

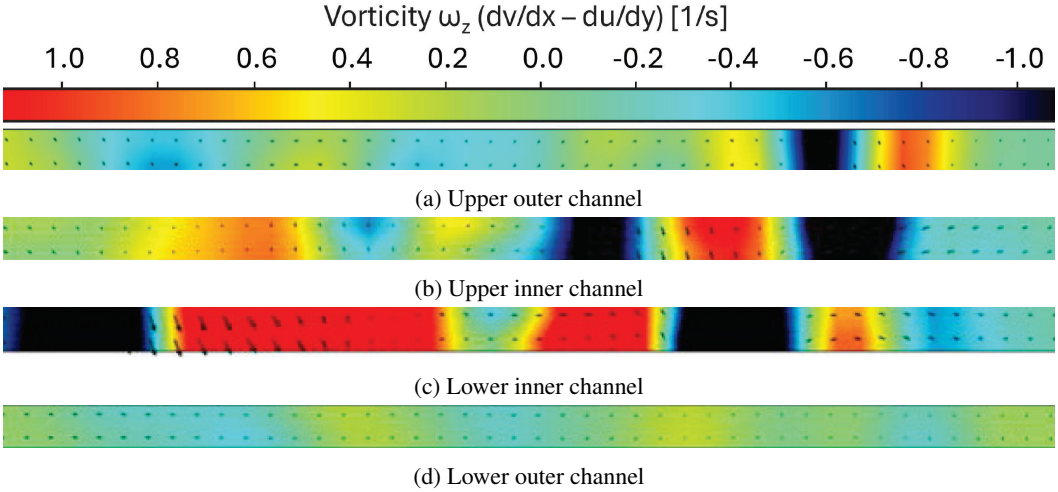

(a) Upper outer channel

(b) Upper inner channel

(c) Lower inner channel

(d) Lower outer channel

Fig. 5 Fine-scale reconstruction of the 20.3 Hz traveling wave, showing inner and outer regions of the upper and lower channels.

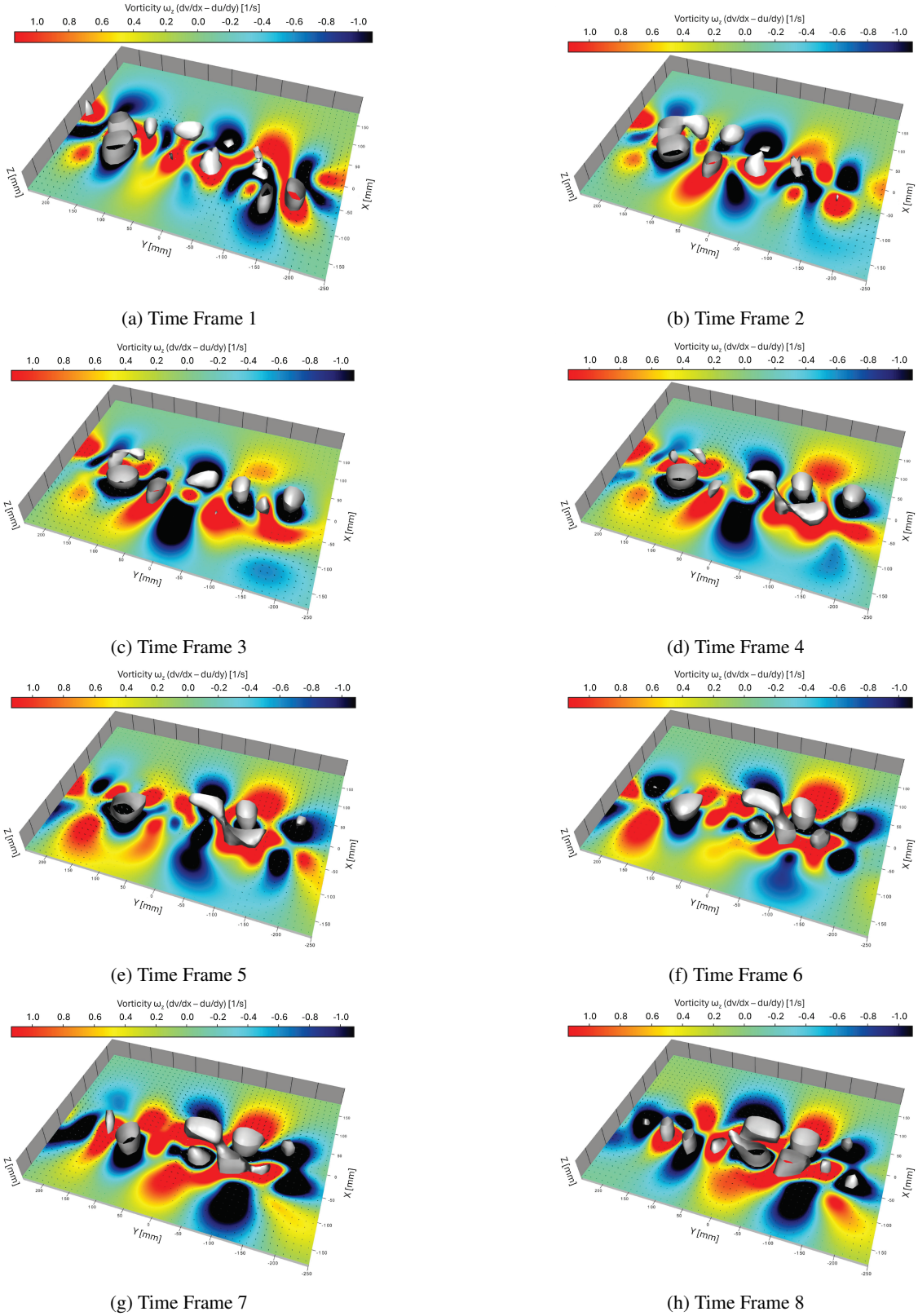

(a) Time Frame 1

(b) Time Frame 2

(c) Time Frame 3

(d) Time Frame 4

(e) Time Frame 5

(f) Time Frame 6

(g) Time Frame 7

(h) Time Frame 8

Fig. 6 Fine-scale reconstruction of the 20.3 Hz traveling wave, showing iso-surfaces across time.

The PTV results demonstrate that two-shaker excitation of a beam in water can generate traveling waves. In the channel configuration, the traveling wave excitation induced vortex structures whose linear momentum resulted in a sustained circular flow throughout the channel system.

Conclusion

Previous studies have reported fluid and particle motion induced by traveling waves, but the mechanisms underlying this motion remain poorly understood. The present experimental model provides a framework for developing a fluid–structure interaction (FSI) model to examine how structure-borne traveling waves couple with the surrounding fluid and drive flow. The fine-scale reconstruction reveals the formation of vortices around the beam. Close inspection over time shows alternating vortices propagating along the beam in the y-direction, producing linear motion in the outer channels. A sequence of eight frames from the dataset is presented in Figure 6 to illustrate this dynamic evolution.

Analysis of the reconstructions further indicates a clear relationship between the traveling wave wavelength and vortex formation: approximately four vortices are generated per excitation wavelength. This observation highlights the role of traveling waves in organizing flow structures and motivates further investigation into FSI models to better characterize vortex number, propagation speed, and related phenomena.

Acknowledgments The author (RC) gratefully acknowledges support from the DoD through the DoD SMART Scholarship. The authors (VVNSM and SG) also acknowledge support from the National Science Foundation under grant CMMI-2301776 for funding the research presented in this paper.

Declaration of generative AI and AI-assisted technologies in the writing process

While preparing this work, the author(s) used ChatGPT to edit the language. After using this tool/service, the author(s) reviewed and edited the content as needed and take(s) full responsibility for the publication's content.

References

1. Liu, Y., Zhu, Y., and Cui, Y. "Challenges and opportunities towards fast-charging battery materials". *Nature Energy*, 4(7):540–550 (2019).
2. Keyser, M., Pesaran, A., Li, Q., Santhanagopalan, S., Smith, K., Wood, E., Ahmed, S., Bloom, I., Dufek, E., Shirk, M., et al. "Enabling fast charging–battery thermal considerations". *Journal of Power Sources*, 367:228–236 (2017).
3. Xu, K. "Nonaqueous liquid electrolytes for lithium-based rechargeable batteries". *Chemical reviews*, 104(10):4303–4418 (2004).
4. Lin, D., Liu, Y., and Cui, Y. "Reviving the lithium metal anode for high-energy batteries". *Nature nanotechnology*, 12(3):194–206 (2017).
5. Olabi, A., Maghrabie, H.M., Adhari, O.H.K., Sayed, E.T., Yousef, B.A., Salameh, T., Kamil, M., and Abdelkareem, M.A. "Battery thermal management systems: Recent progress and challenges". *International Journal of Thermofluids*, 15:100171 (2022).
6. Spotnitz, R. and Franklin, J. "Abuse behavior of high-power, lithium-ion cells". *Journal of power sources*, 113(1):81–100 (2003).
7. Al Hallaj, S. and Selman, J. "A novel thermal management system for electric vehicle batteries using phase-change material". *Journal of the Electrochemical Society*, 147(9):3231 (2000).
8. Kong, L., Li, C., Jiang, J., and Pecht, M.G. "Li-ion battery fire hazards and safety strategies". *Energies*, 11(9):2191 (2018).
9. Lu, L., Han, X., Li, J., Hua, J., and Ouyang, M. "A review on the key issues for lithium-ion battery management in electric vehicles". *Journal of power sources*, 226:272–288 (2013).
10. Wang, Q., Ping, P., Zhao, X., Chu, G., Sun, J., and Chen, C. "Thermal runaway caused fire and explosion of lithium ion battery". *Journal of power sources*, 208:210–224 (2012).
11. Choi, Y.S. and Kang, D.M. "Prediction of thermal behaviors of an air-cooled lithium-ion battery system for hybrid electric vehicles". *Journal of Power Sources*, 270:273–280 (2014).
12. Bandhauer, T.M., Garimella, S., and Fuller, T.F. "A critical review of thermal issues in lithium-ion batteries". *Journal of the electrochemical society*, 158(3):R1 (2011).
13. Yang, N., Zhang, X., Li, G., and Hua, D. "Assessment of the forced air-cooling performance for cylindrical lithium-ion battery packs: A comparative analysis between aligned and staggered cell arrangements". *Applied thermal engineering*, 80:55–65 (2015).
14. Sabbah, R., Kizilel, R., Selman, J., and Al-Hallaj, S. "Active (air-cooled) vs. passive (phase change material) thermal management of high power lithium-ion packs: Limitation of temperature rise and uniformity of temperature distribution". *Journal of power sources*, 182(2):630–638 (2008).
15. Pesaran, A., Keyser, M., and Burch, S. "An approach for designing thermal management systems for electric and hybrid vehicle battery packs". Technical report, National Renewable Energy Laboratory, Golden, CO (US) (1999).
16. Deng, Y., Feng, C., Zhu, H., Chen, J., Wen, M., Yin, H., et al. "Effects of different coolants and cooling strategies on the cooling performance of the power lithium ion battery system: A review". *Applied Thermal Engineering*, 142:10–29 (2018).
17. Roe, C., Feng, X., White, G., Li, R., Wang, H., Rui, X., Li, C., Zhang, F., Null, V., Parkes, M., et al. "Immersion cooling for lithium-ion batteries–a review". *Journal of Power Sources*, 525:231094 (2022).

18. Rao, Z. and Wang, S. "A review of power battery thermal energy management". *Renewable and Sustainable Energy Reviews*, 15(9):4554–4571 (2011).
19. Bernardi, D., Pawlikowski, E., and Newman, J. "A general energy balance for battery systems". *Journal of the electrochemical society*, 132(1):5 (1985).
20. Chen, D., Jiang, J., Kim, G.H., Yang, C., and Pesaran, A. "Comparison of different cooling methods for lithium ion battery cells". *Applied thermal engineering*, 94:846–854 (2016).
21. Fan, S. and Duan, F. "A review of two-phase submerged boiling in thermal management of electronic cooling". *International Journal of Heat and Mass Transfer*, 150:119324 (2020).
22. Ataur, R., Hawlader, M.N.A., and Khalid, H. "Two-phase evaporative battery thermal management technology for evs/hevs". *International journal of automotive technology*, 18(5):875–882 (2017).
23. Shen, M. and Gao, Q. "System simulation on refrigerant-based battery thermal management technology for electric vehicles". *Energy Conversion and Management*, 203:112176 (2020).
24. Zolot, M., Pesaran, A.A., and Mihalic, M. "Thermal evaluation of toyota prius battery pack". Technical report, SAE Technical paper (2002).
25. Zolot, M.D., Kelly, K., Keyser, M., Mihalic, M., Pesaran, A., and Hieronymus, A. "Thermal evaluation of the honda insight battery pack". Technical report, National Renewable Energy Lab.(NREL), Golden, CO (United States) (2001).
26. Kelly, K.J., Mihalic, M., and Zolot, M. "Battery usage and thermal performance of the toyota prius and honda insight during chassis dynamometer testing". In *Seventeenth Annual Battery Conference on Applications and Advances. Proceedings of Conference (Cat. No. 02TH8576)*, pages 247–252. IEEE (2002).
27. Ji, Y. and Wang, C.Y. "Heating strategies for li-ion batteries operated from subzero temperatures". *Electrochimica Acta*, 107:664–674 (2013).
28. Wang, Q., Jiang, B., Li, B., and Yan, Y. "A critical review of thermal management models and solutions of lithium-ion batteries for the development of pure electric vehicles". *Renewable and sustainable energy reviews*, 64:106–128 (2016).
29. Pambudi, N.A., Sarifudin, A., Firdaus, R.A., Ulfa, D.K., Gandidi, I.M., and Romadhon, R. "The immersion cooling technology: Current and future development in energy saving". *Alexandria Engineering Journal*, 61(12):9509–9527 (2022).
30. Murshed, S.S. and De Castro, C.N. "A critical review of traditional and emerging techniques and fluids for electronics cooling". *Renewable and Sustainable Energy Reviews*, 78:821–833 (2017).
31. Khalaj, A.H. and Halgamuge, S.K. "A review on efficient thermal management of air-and liquid-cooled data centers: From chip to the cooling system". *Applied energy*, 205:1165–1188 (2017).
32. Pesaran, A. and Kim, G. "Battery thermal management system design modeling". Technical report, National Renewable Energy Lab.(NREL), Golden, CO (United States) (2006).
33. Neighborgall, C.R., Kothari, K., Sriram Malladi, V., Tarazaga, P., Paruchuri, S.T., and Kurdila, A. "Shaping the frequency response function (frf) of a multi-degree-of-freedom (mdof) structure using arrays of tuned vibration absorbers (tva)". In *Topics in Modal Analysis & Testing, Volume 8: Proceedings of the 37th IMAC, A Conference and Exposition on Structural Dynamics 2019*, pages 317–326. Springer (2019).
34. Paruchuri, S.T., Sterling, J., Malladi, V.V.S., Kurdila, A., Vignola, J., and Tarazaga, P. "Passive piezoelectric subordinate oscillator arrays". *Smart Materials and Structures*, 28(8):085046 (2019).
35. Sterling, J., Paruchuri, S.T., Tarazaga, P., Vignola, J., Kurdila, A., Malladi, V.V.S., and Ryan, T. "Piezoelectric subordinate oscillator arrays: Performance recovery and robustness to uncertainty". In *International Design Engineering Technical Conferences and Computers and Information in Engineering Conference*, volume 59285, page V008T10A043. American Society of Mechanical Engineers (2019).
36. Wang, Y. and Inman, D.J. "A survey of control strategies for simultaneous vibration suppression and energy harvesting via piezoceramics". *Journal of Intelligent Material Systems and Structures*, 23(18):2021–2037 (2012).
37. Sodano, H.A., Inman, D.J., and Park, G. "A review of power harvesting from vibration using piezoelectric materials". *Shock and Vibration Digest*, 36(3):197–206 (2004).
38. Junior, C.D.M., Erturk, A., and Inman, D.J. "An electromechanical finite element model for piezoelectric energy harvester plates". *Journal of Sound and Vibration*, 327(1-2):9–25 (2009).
39. Erturk, A. and Inman, D.J. *Piezoelectric energy harvesting*. John Wiley & Sons (2011).
40. Priya, S. "Advances in energy harvesting using low profile piezoelectric transducers". *Journal of electroceramics*, 19(1):167–184 (2007).
41. Zabek, D., Taylor, J., Ayel, V., Bertin, Y., Romestant, C., and Bowen, C. "A novel pyroelectric generator utilising naturally driven temperature fluctuations from oscillating heat pipes for waste heat recovery and thermal energy harvesting". *Journal of Applied Physics*, 120(2) (2016).
42. Chiolerio, A., Garofalo, E., Mattiussi, F., Crepaldi, M., Fortunato, G., and Iovieno, M. "Waste heat to power conversion by means of thermomagnetic hydrodynamic energy harvester". *Applied Energy*, 277:115591 (2020).
43. Suo, G., Yu, Y., Zhang, Z., Wang, S., Zhao, P., Li, J., and Wang, X. "Piezoelectric and triboelectric dual effects in mechanical-energy harvesting using batio3/polydimethylsiloxane composite film". *ACS applied materials & interfaces*, 8(50):34335–34341 (2016).
44. Lang, S.B. "Pyroelectricity: from ancient curiosity to modern imaging tool". *Physics today*, 58(8):31–36 (2005).
45. Bowen, C.R., Taylor, J., LeBoulbar, E., Zabek, D., Chauhan, A., and Vaish, R. "Pyroelectric materials and devices for energy harvesting applications". *Energy & Environmental Science*, 7(12):3836–3856 (2014).
46. Barbier, E. "Geothermal energy technology and current status: an overview". *Renewable and sustainable energy reviews*, 6(1-2):3–65 (2002).
47. Avirovik, D., Kumar, A., Bodnar, R.J., and Priya, S. "Remote light energy harvesting and actuation using shape memory alloy—piezoelectric hybrid transducer". *Smart Materials and Structures*, 22(5):052001 (2013).
48. Avirovik, D., Kishore, R.A., Vuckovic, D., and Priya, S. "Miniature shape memory alloy heat engine for powering wireless sensor nodes". *Energy Harvesting and Systems*, 1(1-2):13–18 (2014).
49. Bai, S. and Liu, C. "Overview of energy harvesting and emission reduction technologies in hybrid electric vehicles". *Renewable and Sustainable Energy Reviews*, 147:111188 (2021).
50. Aksu, U. and Halicioglu, R. "A review study on energy harvesting systems for vehicles". *Tehnički glasnik*, 12(4):251–259 (2018).
51. Li, D., Wu, Y., Da Ronch, A., and Xiang, J. "Energy harvesting by means of flow-induced vibrations on aerospace vehicles". *Progress in Aerospace Sciences*, 86:28–62 (2016).

52. Hewawasam, L., Jayasena, A., Afnan, M., Ranasinghe, R., and Wijewardane, M. "A review paper on use of thermo-electric materials for future energy harvesting in automobile sector". In *2018 8th International Conference on Power and Energy Systems (ICPES)*, pages 157–160. IEEE (2018).
53. Maurya, D., Kumar, P., Khaleghian, S., Sriramdas, R., Kang, M.G., Kishore, R.A., Kumar, V., Song, H.C., Park, J.M.J., Taheri, S., et al. "Energy harvesting and strain sensing in smart tire for next generation autonomous vehicles". *Applied energy*, 232:312–322 (2018).
54. Anton, S.R. and Sodano, H.A. "A review of power harvesting using piezoelectric materials (2003–2006)". *Smart materials and Structures*, 16(3):R1 (2007).
55. Malladi, V.V.S., Albakri, M., Musgrave, P., and Tarazaga, P.A. "Investigation of propulsive characteristics due to traveling waves in continuous finite media". In *Bioinspiration, Biomimetics, and Bioreplication 2017*, volume 10162, pages 112–119. SPIE (2017).
56. Musgrave, P.F., Albakri, M.I., Tenney, C., and Tarazaga, P.A. "Generating and tailoring structure-borne traveling waves on two-dimensional surfaces". *Journal of Sound and Vibration*, 480:115417 (2020).
57. Sfakiotakis, M., Lane, D.M., and Davies, J.B.C. "Review of fish swimming modes for aquatic locomotion". *IEEE Journal of oceanic engineering*, 24(2):237–252 (2002).
58. Anakok, I., Malladi, V.S., and Tarazaga, P.A. "A theoretical study on the generation and propagation of traveling waves in strings". In *Topics in Modal Analysis & Testing, Volume 8: Proceedings of the 37th IMAC, A Conference and Exposition on Structural Dynamics 2019*, pages 311–316. Springer (2019).
59. Phoenix, A., Malladi, V.S., and Tarazaga, P.A. "Traveling wave phenomenon through piezoelectric actuation of a free-free cylindrical tube". In *Smart Materials, Adaptive Structures and Intelligent Systems*, volume 57304, page V002T04A018. American Society of Mechanical Engineers (2015).
60. Anakok, I., Malladi, V.S., and Tarazaga, P.A. "A study on the generation and propagation of traveling waves in strings". In *Topics in Modal Analysis & Testing, Volume 9: Proceedings of the 36th IMAC, A Conference and Exposition on Structural Dynamics 2018*, pages 257–261. Springer (2018).
61. Anakok, I., Davaria, S., Tarazaga, P.A., and Malladi, V.V.S. "A study on steady-state traveling waves in one-dimensional non-dispersive finite media". *Journal of Sound and Vibration*, 528:116907 (2022).
62. Avirovik, D., Malladi, V.S., Priya, S., and Tarazaga, P.A. "Theoretical and experimental correlation of mechanical wave formation on beams". *Journal of Intelligent Material Systems and Structures*, 27(14):1939–1948 (2016).
63. Malladi, V.V.N.S. "Continual traveling waves in finite structures: theory, simulations, and experiments" (2016).
64. Malladi, V.S., Avirovik, D., Priya, S., and Tarazaga, P.A. "Travelling wave phenomenon through a piezoelectric actuation on a free-free beam". In *Smart Materials, Adaptive structures and intelligent systems*, volume 46148, page V001T03A017. American Society of Mechanical Engineers (2014).
65. Malladi, V., Avirovik, D., Priya, S., and Tarazaga, P. "Characterization and representation of mechanical waves generated in piezo-electric augmented beams". *Smart Materials and Structures*, 24(10):105026 (2015).
66. Malladi, V.S., Albakri, M., Tarazaga, P.A., and Gugercin, S. "Reduced plate model used for 2d traveling wave propagation". In *Smart Materials, Adaptive Structures and Intelligent Systems*, volume 57298, page V001T03A021. American Society of Mechanical Engineers (2015).
67. Malladi, V.V.S., Albakri, M., and Tarazaga, P.A. "An experimental and theoretical study of two-dimensional traveling waves in plates". *Journal of Intelligent Material Systems and Structures*, 28(13):1803–1815 (2017).
68. Musgrave, P.F., Sriram Malladi, V., and Tarazaga, P.A. "Generation of traveling waves in a 2d plate for future drag reduction manipulation". In *Special Topics in Structural Dynamics, Volume 6: Proceedings of the 34th IMAC, A Conference and Exposition on Structural Dynamics 2016*, pages 129–138. Springer (2016).
69. Musgrave, P.F. and Tarazaga, P.A. "Turbulent boundary layer over a piezoelectrically excited traveling wave surface". In *AIAA Scitech 2019 Forum*, page 1354 (2019).
70. Krishnan, M., Malladi, V.V.S., and Tarazaga, P.A. "Leveraging a data-driven approach to simulate and experimentally validate a mimo multiphysics vibroacoustic system". *Mechanical Systems and Signal Processing*, 166:108414 (2022).
71. Davaria, S., Krishnan, M., Sriram Malladi, V.V., and Tarazaga, P.A. "Miniature underwater robot–an experimental case study". In *Special Topics in Structural Dynamics & Experimental Techniques, Volume 5: Proceedings of the 40th IMAC, A Conference and Exposition on Structural Dynamics 2022*, pages 119–122. Springer (2022).
72. Avitabile, P. *Modal testing: a practitioner's guide*. John Wiley & Sons (2017).
73. Bucher, I. "Estimating the ratio between travelling and standing vibration waves under non-stationary conditions". *Journal of sound and vibration*, 270(1-2):341–359 (2004).
74. Gadekar, S.S. "An experimental study towards underwater propulsion system using structure borne traveling waves". Master's thesis, Michigan Technological University (2022).
75. Gupta, S. and Malladi, V.V.S. "Utilizing steady-state traveling waves in a quiescent water environment for particle propulsion". In *Smart Materials, Adaptive Structures and Intelligent Systems*, volume 88322, page V001T03A008. American Society of Mechanical Engineers (2024).